

TOHOKU BUBBLE CHAMBER MAGNET
FIELD CALCULATIONS

W. Craddock
January 21, 1985

Introduction

In the early stages of design, Bob Lari (ANL) and Eddie Leung made some preliminary magnetic field calculations using both TRIM and GFUN. GFUN (3D) was abandoned as having not enough iron elements for proper convergence. SLAC ran some NUTCRACKER calculations on the old conventional copper coils using a course 2" uniform mesh which did not fully converge. Most all of the magnetic field design is based on subsequent cylindrical TRIM runs attempting to model our 3D problem. Half way through construction the new Tohoku Bubble Chamber was proposed. Major changes in the iron were required and are listed below.

1. Bore was increased from 40.075" to 45.231".
2. The iron was shimmed apart at the midplane by an additional 3". (The distance from iron face to iron face increased from 44" to 47").
3. Large notches, 5" on each iron half, were machined out to provide a path for muons if required.
4. The iron bridges on the top holding the chamber were modified.

Axial magnetic forces on the coil were a primary design concern. At some arbitrarily high current any coil/iron system of this type will experience a force reversal where the coils are attracted to one another. Our support system design requires that this never happens. On the other hand, the coils must be located so that the axial force towards the iron is not excessive. Many of the "old" iron preliminary design calculations will be listed to give a feel for the axial force sensitivity to coil location, shape, and current.

Figures 1 and 2 show the "old" iron, and the "new" iron with the 3" midplane spacer plates and muon notches. Underlined numbers on these two figures refer to the various areas. The muon notches are capable of being completely filled back in with iron. For the first run the muon notches will be filled 6" deep in each of the four corners with 1018 steel. The top pieces will be 32.375" long and the bottom pieces 49" long. The bulk of the iron yoke is made from 1008 steel.

Axisymmetric TRIM Calculations

Different TRIM meshes were used for the cylindrical approximations to the original iron and the present iron. In both cases a B-H curve for 1010 steel was used. Except for the 3" midplane spacers all of the Tohoku Magnet iron is 1008 steel. This is expected to make little difference. TRIM 5000 was used for the

original iron, and TRIMIOKSC was used for the final iron. Figure 3 is the mesh for the "old" iron and Fig. 4 is the mesh for the "new" iron. Figure 5 is a simplified sketch of the "old" iron and generalized coil dimensions. This figure also shows the location of the original copper coils.

"Old" iron calculations assume that no flux jumped across the 12" wide beam window areas. At full current 2×10^6 amps per coil the average flux in the return leg is 14 kG. This far below saturation and justifies the neglect of the air gap. From Fig. 1,

$$\text{Area touching across midplane} = 6728 + 168 = 6896 \text{ in}^2$$

where 168 in² is the contribution from the iron bridges (not shown).

$$\text{Area of return leg is TRIM model} = \pi(65.61^2 - 45.25^2) = 7091 \text{ in}^2$$

This area is 3% greater than the actual area and included some obsolete beam window iron filler plates. The difference in fields will be very small.

Table 1 is a summary of the various coil geometries which were tried during the initial design. Run #32 was the original copper coil comparison. Figure 6 is a flux plot for these coils at 2×10^6 amp turns per coil. Flux density plots for the cylindrical version of TRIM are multiplied by the radius. At 1.47×10^6 amps per coil, TRIM run #32 gives a central field of $B_0 = 25,046$ kG. Bill Bugg from the University of Tennessee measured a field of $B_0 = 25.01$ kG at location ($x = 0.276$ ", $y = 0.078$ ", $z = -0.51$ ") with an NMR probe at a current of 14,700 amps = 1.47×10^6 amp turns. There were 25 turns in each of 4 double pancakes in both of the original copper coils. Bill Bugg's location is essentially the center. For TRIM #32 at $r = 0.0$ " and $z = 0.5$ ", $B_z = 25.044$ kG. The comparison between the calculated value and measured value is excellent. This accuracy is not expected for the new modified iron with unfilled muon notches as the iron in the return legs is saturated and the cylindrical approximation to the 3D geometry is not as close.

In Table 1 note also runs #12 and #20. With μ iron the axial force is 1.2×10^6 lbs, and with coils only the force is -6.33×10^5 lbs. This is to be compared with a finite μ iron run #8 of $F_z = 2.26 \times 10^5$ lbs. All three runs have the same coil geometry and current.

Figure 7 is a sketch of the TRIM model of the final iron and coil dimensions. The coil is located between $r = 25.14$ " and 33.27 " with the center 6.978 " away from the iron face. The nominal warm location is 7.000 ". Final coil position was based on 0.014 " change from cooldown plus 0.009 " support compression from a 125,000 lb axial load. Radial positions are 4.2 K locations.

From Fig. 2,

$$\text{Area touching at midplane } (\mu \text{ notch unfilled}) = 2409 + 89 = 2498 \text{ in}^2$$

$$\text{Area of muon notch (13" midplane gap)} = 4189 \text{ in}^2$$

$$\text{Area of beam windows (15" midplane gap)} = 2554 \text{ in}^2$$

TABLE 1

 AXIAL COIL FORCES
 OLD IRON/TRIM 5000

Run #	$\times 10^6$ Amps	R_i	R_0	Z_{min}	Z_{max}	Z_{center}	Fz (lbs)	Comments
Run Trim	2.0	29.875	36.0	9.5	18.5	14.0	+97,400	Initial run by B. Lari (ANL)
Run Trim 2	2.0	29.875	36.0	9.5	18.5	14.0	+97,400	Start of Fermilab runs
5	2.0	21.875	32.0	9.5	18.5	14.0	-78,160	91.1 sq. in.
4	2.0	21.875	32.0	10.0	19.0	14.5	+ 4,400	
13	1.4	21.875	32.0	10.0	19.0	14.5	+94,400	
16	1.0	21.875	32.0	10.0	19.0	14.5	+94,170	
16	0.7	21.875	32.0	10.0	19.0	14.5	+64,900	
13	2.5	21.875	32.0	10.0	19.0	14.5	-145,000	
6	2.0	21.875	32.0	11.0	20.0	15.5	1.77×10^5	
6	2.0	22.25	29.75	8.0	20.0	14.0	-9.1×10^4	Rectangular coil $\square \uparrow z$
10	2.0	25.25	35.25	8.5	17.5	13.0	-1.96×10^5	90.0 sq. in.
7	2.0	25.25	35.25	9.5	18.5	14.0	+12,860	
31	2.0	25.25	33.75	10.5	19.5	15.0	2.04×10^5	
8	2.0	25.25	35.25	10.5	19.5	15.0	2.26×10^5	
12	2.0	25.25	35.25	10.5	19.5	15.0	1.21×10^6	$\infty \mu$ iron
17	1.5	25.25	35.25	10.5	19.5	15.0	2.64×10^5	
17	1.0	25.25	35.25	10.5	19.5	15.0	2.097×10^5	
18	0.5	25.25	35.25	10.5	19.5	15.0	74,700	
18	2.5	25.25	35.25	10.5	19.5	15.0	1.14×10^5	
20	2.0	25.25	35.25	10.5	19.5	15.0	-6.33×10^5	Air -- no steel
Nut Cracker	2.0	26.0	38.0	10.0	16.0	13.0	-1.90×10^5	SLAC -2" Mesh- Not Fully converged
TRIM 15	2.0	26.0	38.0	10.0	16.0	13.0	-1.505×10^5	Comparison - 1/2" mesh
15	2.5	26.0	38.0	10.0	16.0	13.0	-4.58×10^5	
14	1.2	26.0	38.0	10.0	16.0	13.0	75,170	
32	2.0	20.25	45.25	6.0	22.0	14.0	9.09×10^4	Original copper water cooled coils
32	1.47	20.25	45.25	6.0	22.0	14.0	1.75×10^5	

NOTE: Positive force is coils that are attracted towards iron.

Area touching at midplane with completely filled muon notches
 $= 2498 + 4189 = 6687 \text{ in}^2$

Area touching at midplane with first run 6" deep corner muon fill
 bars $= 2398 + 978 = 3476 \text{ in}^2$. Then area of unfilled muon notch
 $= 4189 - 978 = 3211 \text{ in}^2$.

TRIM model areas,

Area always touching at midplane $= \pi(53.858^2 - 45.25^2) = 2680 \text{ in}^2$

Area of muon notch $= \pi(65.0^2 - 53.858^2) = 4160 \text{ in}^2$

Area of beam windows $= \pi(71.0^2 - 65.0^2) = 2564 \text{ in}^2$

The areas of the muon notches and beam windows were chosen very slightly differently to allow a "nicer" mesh. By mistake the area permanently touching is 7% greater than the actual area. This would cause some differences at the high field range. A single 2" thick muon notch plate in each of the four corners will provide 326 in^2 of area at the midplane for a total of 2824 in^2 or 5% greater area than the TRIM run with the unfilled notch. Our initial run uses three 2" fill bars in each of the corners.

Table 2 lists the axial forces for the final coil/iron configurations with central field, stored energy, inductance and return leg flux values. Surprisingly little difference is found in central fields, stored energies or axial forces between the filled and unfilled muon notch cases. Figures 8 to 12 show the flux distributions. When the muon notch is completely unfilled, a large percentage of the total flux jumps across the air gap at 2.0×10^6 amp-turns per coil. For the first run with the 6" of muon notch filler plates, the iron is completely saturated at the midplane at full field.

Figure 13 is plots of axial force versus current. The unfilled muon notch case has slightly higher maximum axial force and is less sensitive to force reversal. From a crude extrapolation of the curves, one would not expect force reversal until 2.75×10^6 amp-turns (970 amps) for either case.

Axial force versus coil location are plotted for two "old" iron geometries in Fig. 14. A magnetic spring constant of $\sim 2 \times 10^5$ lbs/inch is found. No spring constant data is available for our final iron configuration, but the results are expected to be very similar.

Table 2
Axial Coil Forces
Final Coil Geometry

Run No.	Fig. Ref.	Current per Coil $\times 10^6$ Amps	F_z lbs	B_0 kG	B† Return Leg kG	Stored Energy MJ	Inductance Henries	Iron Configuration
41	8	1.0	1.72×10^5	15.29	16.5	3.13	50.5	μ notch unfilled
41	--	1.5	2.31×10^5	22.17	21.1	6.66	47.7	μ notch unfilled
41	9	2.0	2.40×10^5	28.67	22.7	11.33	45.7	μ notch unfilled
41	10	2.5	2.10×10^5	35.02	23.6	17.20	44.4	μ notch unfilled
40	--	2.0	1.06×10^6	31.70	--	13.48	54.4	Same as 41 but $\infty \mu$ iron
47	11	1.0	1.71×10^5	15.33	6.6	3.14	50.7	μ notch totally filled
47	--	1.5	2.22×10^5	22.32	9.5	6.72	48.2	μ notch totally filled
47	12	2.0	2.05×10^5	29.04	12.1	11.51	46.4	μ notch totally filled
49	--	1.0	2.655×10^5 2.641×10^5 *	15.82	--	3.36	54.2	Same as 47 but ∞ iron

† This is the average flux in the iron across the midplane.

* All force calculations except this one were made with "old" FORGY. This includes results from Table 1 as well. Forces calculated by $F_x = \Delta A_y / \text{distance} \times \text{current}$ ($B = \nabla \times A$) where ΔA is the difference between vector potentials of two adjacent mesh points and \vec{F} is perpendicular to the line connecting the mesh points. This particular force calculation uses "NEW" FORGY and serves as a check.

NUFORGY is based on a nonweighted average of the B fields in each of the six triangles surrounding every mesh point. It is normally intended for irregular shaped coils. The exact value is unimportant because the axial support system has a stiffness of $\Delta F/\Delta X = AE/L = 1.2 \times 10^7$ lbs/inch or roughly sixty times as great.

Figure 15 plots stored energy versus total amp turns². Iron saturation is already noticeable at 350 amps. A plot of energy versus current² is also provided for the ideal ∞ u iron case as a comparison. Inductances are listed in Table 2, and are seen to fall by 16% between the very low current case (∞ u iron) and 2×10^6 amp turns. Figure 16 plots the magnitude of the magnetic field through the coil at three different axial locations. The maximum magnetic field is found to be 54.1 kG (2×10^6 amp-turns) at the center of the inner radius of the coil. This number is important for stability considerations. Midplane magnetic fields are plotted in Fig. 17.

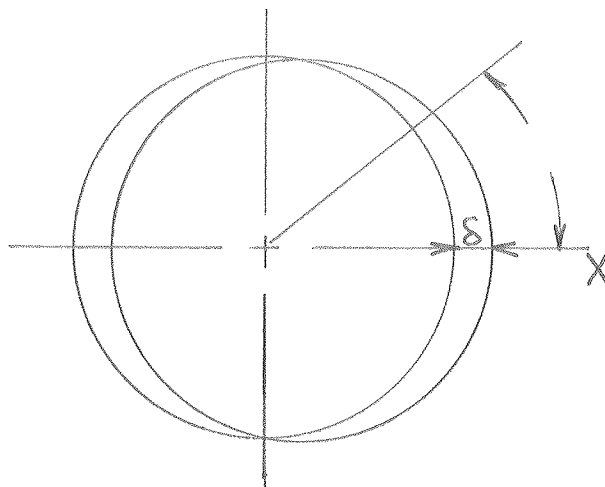
Radial Coil Forces

Radial forces and radial magnet spring constants cannot be estimated as well as the axial components. The iron is highly asymmetric, and the coil will be displaced by 1/8" upward during cooldown. Estimates can be made for the radial spring constant or force by the following methods.

1. Displacement of coil in a fixed background field.
2. Actual field measurements.
3. Assumed field differences.
4. TRIM estimates.
5. Method of images.

Displacement of Coil in a Fixed Background Field:

Take a coil with 2×10^6 amp-turns and displace it an amount δ where δ is much smaller than r . Assuming a fixed background field is provided by the iron and is independent of small coil displacements, the radial magnetic spring constant can be estimated.



$$dF_x = I dl H_z \cos \theta$$

$$H_z = H_{z0} + \frac{\partial H_z}{\partial r} \delta r$$

$$\delta r \sim \delta \cos \theta$$

$$F_x = \int_0^{2\pi} I H_{z0} \cos \theta r d\theta + \int_0^{2\pi} I \frac{\partial H_z}{\partial r} \delta \cos^2 \theta d\theta = I \frac{\partial H_z}{\partial r} \pi \delta r$$

$$\frac{\Delta F_x}{\Delta r} = 0.82 \times 2 \times 10^6 \times 0.2248 \text{ lbs/N} = 3.7 \times 10^5 \text{ lbs/inch per coil}$$

where

$$\frac{\partial H_z}{\partial r} \sim (5.38 - -1.27)/(33.27'' - 25.14'') = 0.82 \text{ Tesla/inch}$$

This magnetic spring constant is much smaller than the mechanical radial spring constants.

Actual Field Measurements:

Close attention must be paid to radial forces which can arise from asymmetries in the iron. These forces are essentially independent of coil location. There is more iron at the bottom of the magnet than at the top and more iron on the upstream side than the downstream side. One would expect that the force on the magnet should be down and towards the upstream end. Bill Bugg and Ed Hart from the University of Tennessee have measured the axial component of the field near the old copper coils and old iron geometry. This should give us a ball park estimate for the superconducting coil and modified iron. See Appendix A. Below is a list of the points measured on the face of one of the coils:

r	θ
30.6"	61°
29.0"	-60°
34.6"	50.5°
32.9"	-51°
20" to 45"	+15° to -15°
20" to 45"	165° to 195°

It was found that the axial field was 4.6% higher at the -60° position when compared with the $+60^\circ$ position. A legendre polynomial expansion of the data points from $+15^\circ$ to -15° and from 165° to 195° was made by Bill Bugg. His estimate of the field difference between 61° and -60° positions agreed within 1/2% of the actual field measured by Ed Hart. Bill Bugg's best estimate of the radial decentering forces at 1.47×10^6 amp-turns per coil is the following:

$$F_z = 75,000 \text{ lbs down}$$

$$F_x = 40,000 \text{ lbs upstream}$$

Assumed Field Differences:

If one were to assume that the axial field was uniformly 5% larger on the bottom half of the magnet than on the top half and that the average axial field in the coil was 3T then,

$$F_r = \int_0^{-180^\circ} 2 \times 10^6 \times (3 \times 0.05) \frac{29.2''}{39.37 \text{ in/m}} \sin \theta \, d\theta$$

$$= 4.45 \times 10^5 \text{ N} = 1.0 \times 10^5 \text{ lbs.}$$

TRIM Estimates:

One computer estimate of the radial decentering force has been made using the geometry shown in Fig. 18. Old coil and iron geometries were used (TRIM 2). The infinitely permeable return path moves the image currents far away from the coils. Actually a B-H curve with large constant μ at all fields was used. The difference in radial attraction between this case and the previous iron geometries shows up as a difference in hoop tension.

This change in hoop tension approximates our actual iron with large amounts of iron removed from the top.

$$F_x = 2 \times \Delta \text{ hoop tension} = 82,000 \text{ lbs per coil at } 2 \times 10^6 \text{ amp-turns}$$

Method of Images:

S. Oh and I. Pless from MIT estimated worse case radial decentering forces using the method of images. See Appendix B. From their study a coil with radius $r = 29''$ in a spherical $\infty\mu$ iron cavity at 1.5×10^6 amps should have a radial spring constant of $\sim 16,700$ lbs/inch. Since forces are proportional to I^2 we should expect 29,700 lbs/inch at full field.

Radial Force Summary:

Estimates of the radial decentering force or spring constant vary widely. From asymmetries in the iron and 1/8" coil affect during cooldown, the vertical decentering force is expected to be by far the largest. This force is accurately and easily measured with four strain gage bolts connected to the vertical stainless steel support arms. The support system was designed for an operating load of 150,000 lbs downward and 75,000 lbs left or right. All of our estimates fall within these two ranges.

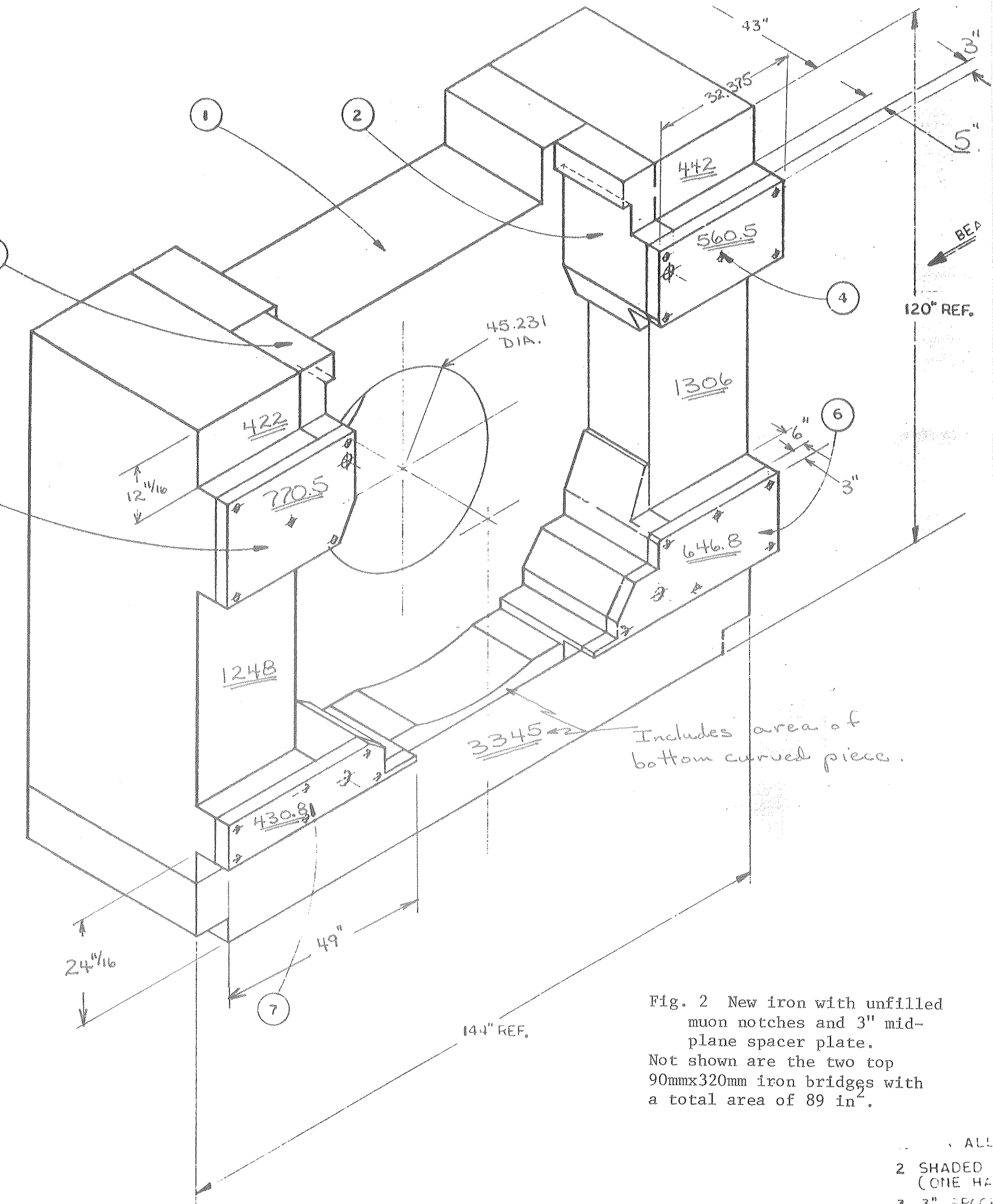


Fig. 2 New iron with unfilled muon notches and 3" mid-plane spacer plate. Not shown are the two top 90mmx320mm iron bridges with a total area of 89 in².

- ALL
- 2 SHADED (ONE HA
- 3. 3" SPACE USED FO
- 4. ALL TAPP 2-1/2 D

Fig. 3 Old Iron Mesh

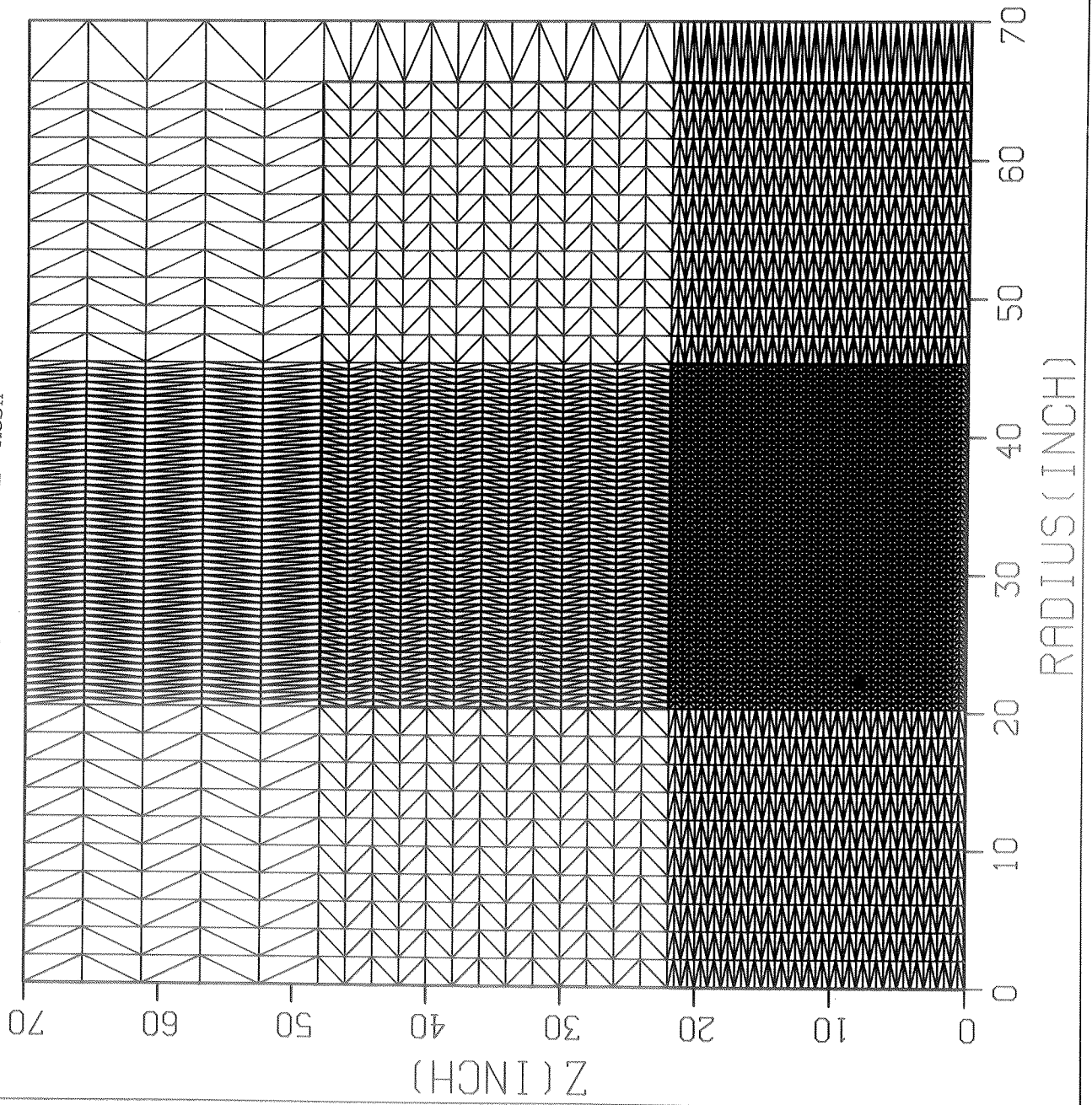
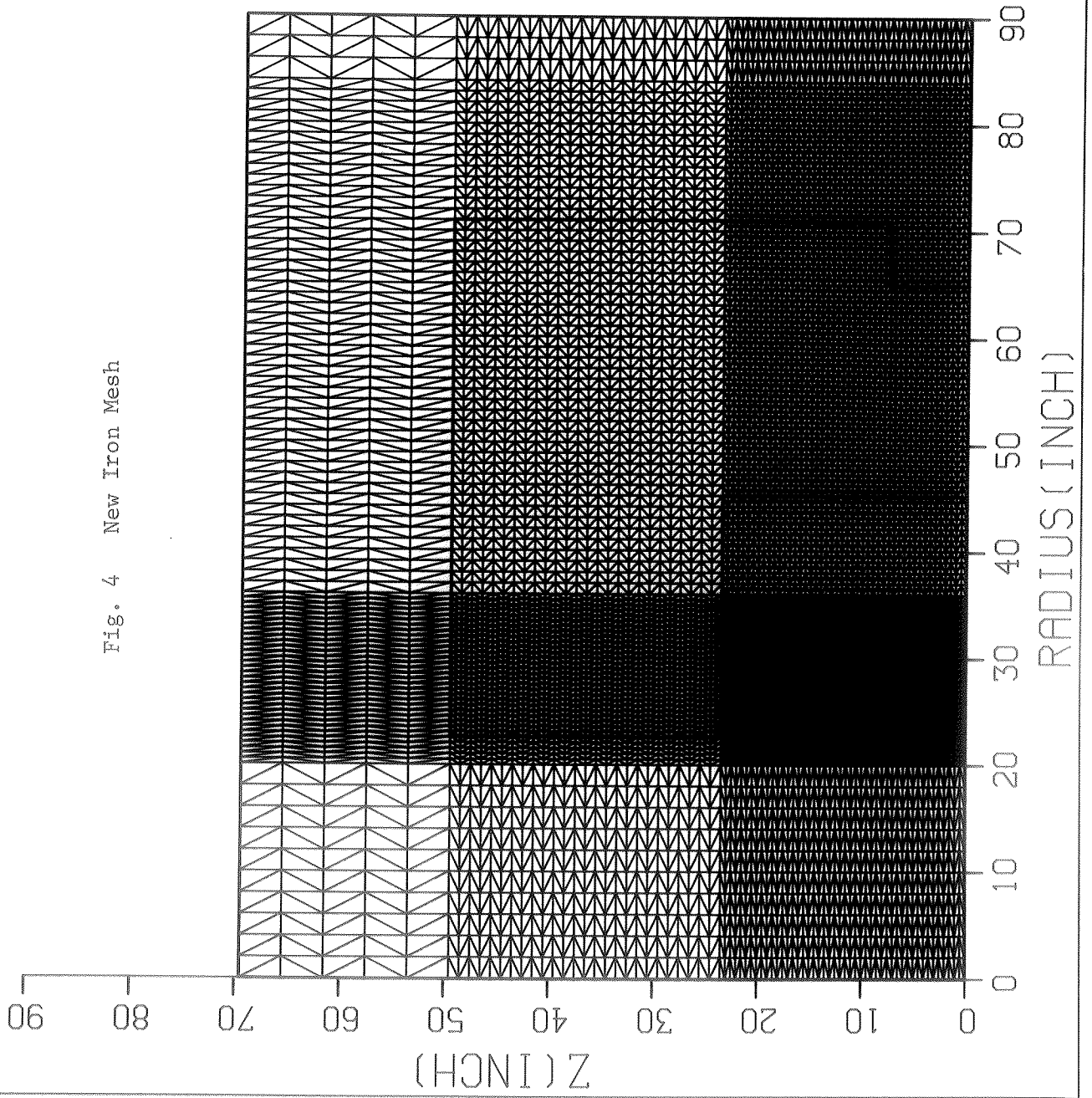


Fig. 4 New Iron Mesh





FERMILAB
ENGINEERING NOTE

SECTION

PROJECT

SERIAL - CATEGORY

PAGE

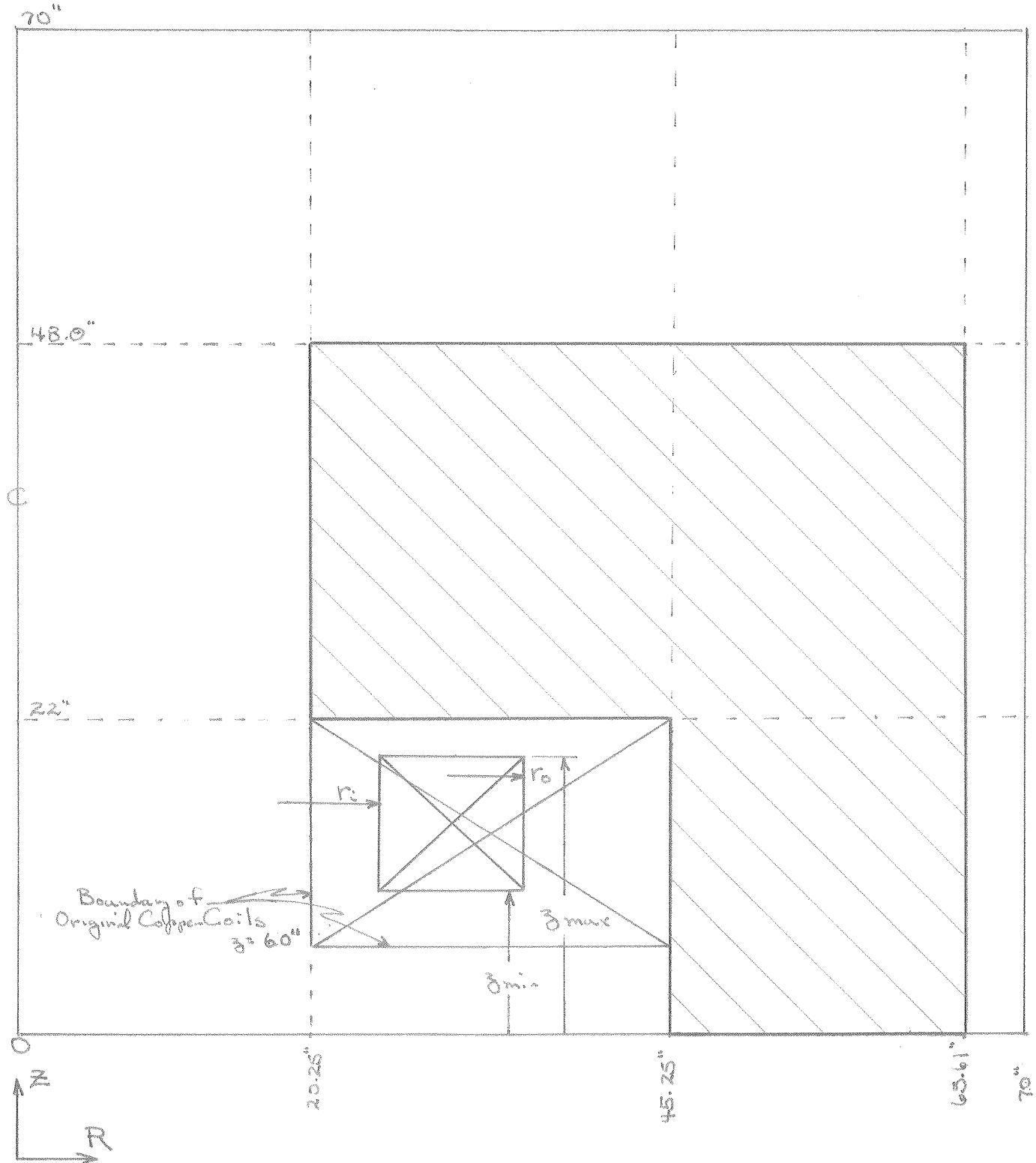
SUBJECT

NAME

DATE

REVISION DATE

Figure 5
"Old" iron with generalized
coil dimensions.



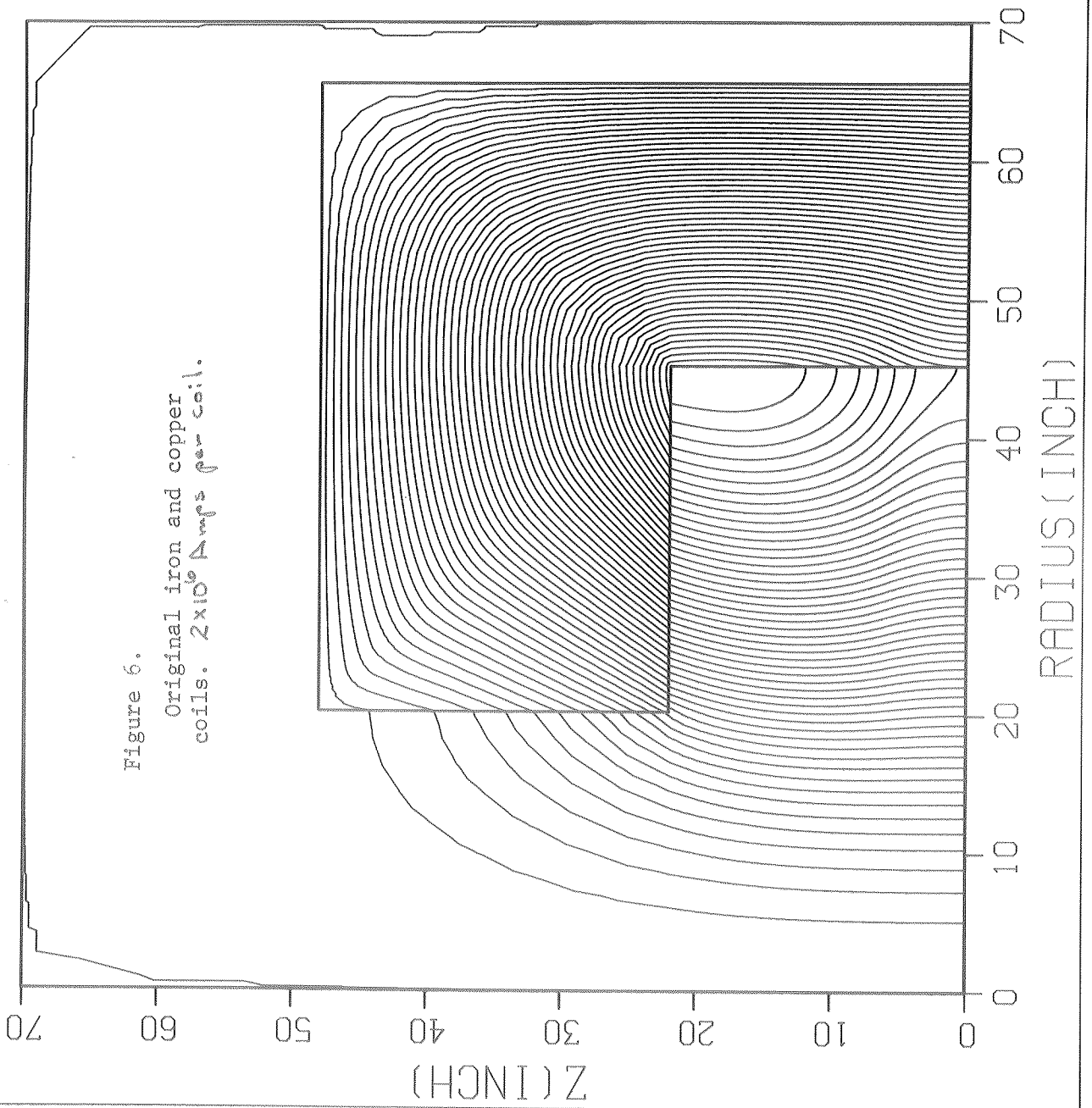


Figure 6.
Original iron and copper
coils. 2×10^6 Amps per coil.

Fig. 8 TRIM run #41
muon notch unfilled
1.0 x 10⁶ amps

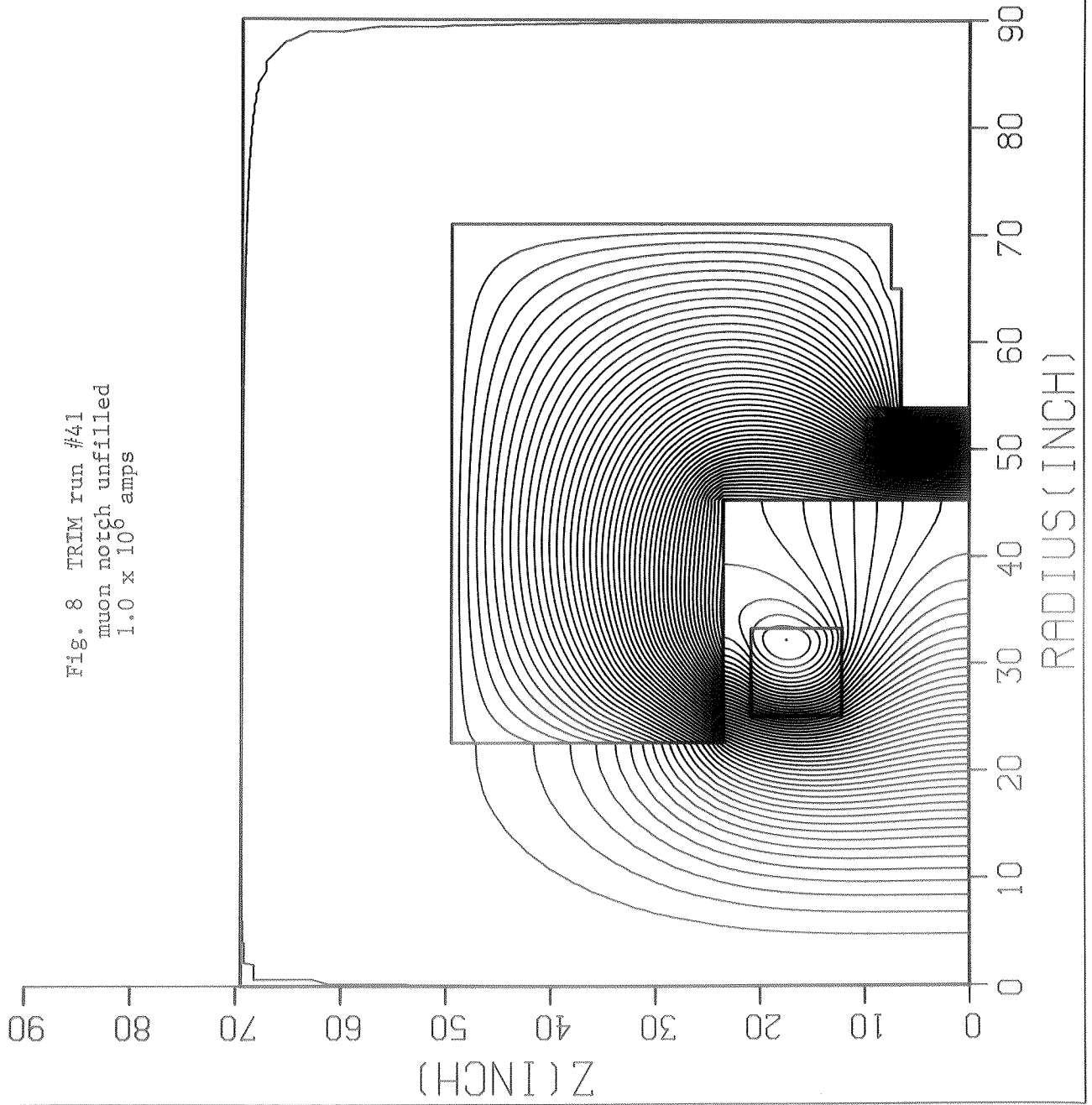


Fig.9 TRIM run #41
muon notch unfilled
2.0 x 10⁶ amps

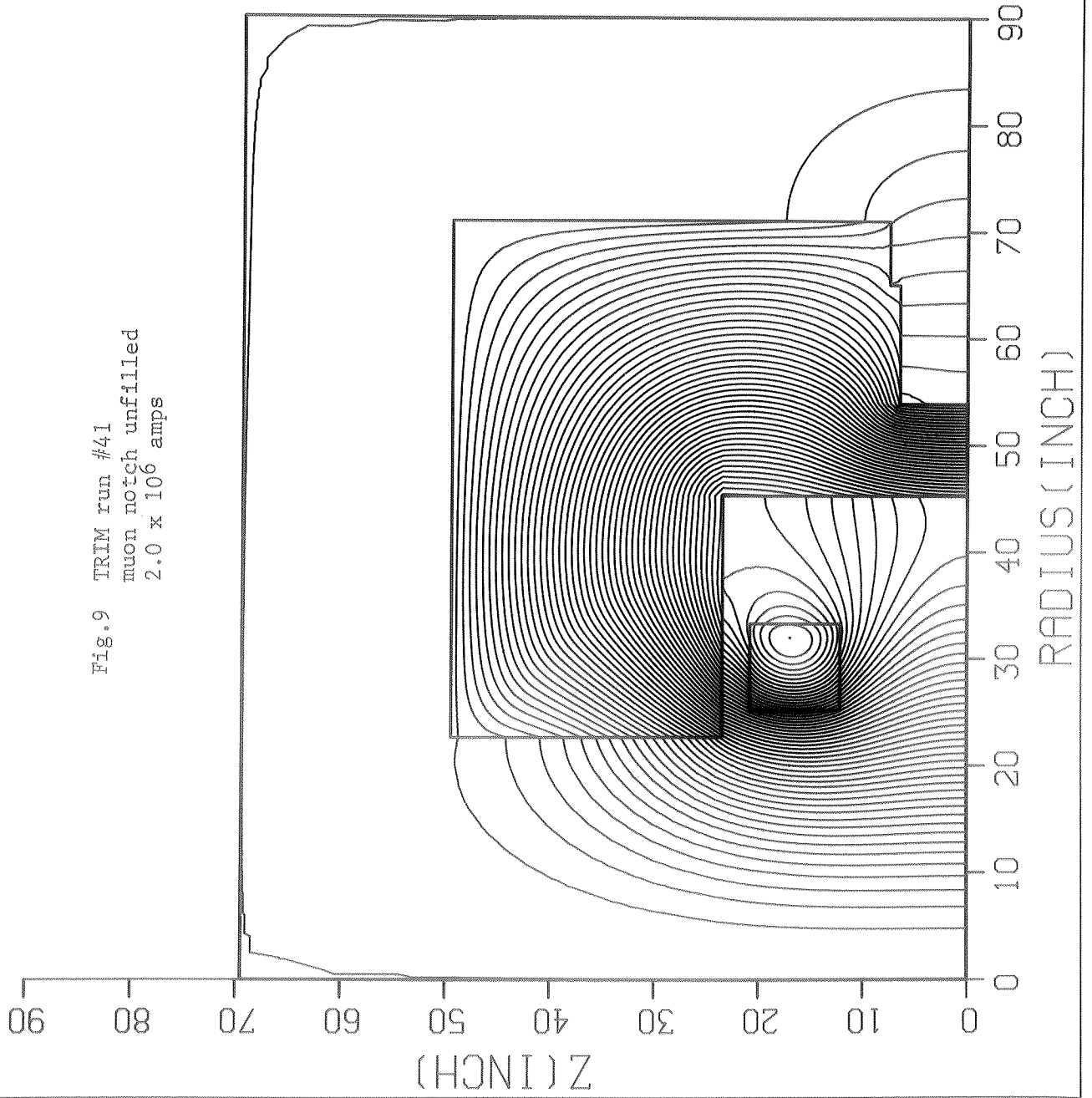


Fig. 10 TRIM run #41
muon notch unfilled
2.5 x 10⁶ amps

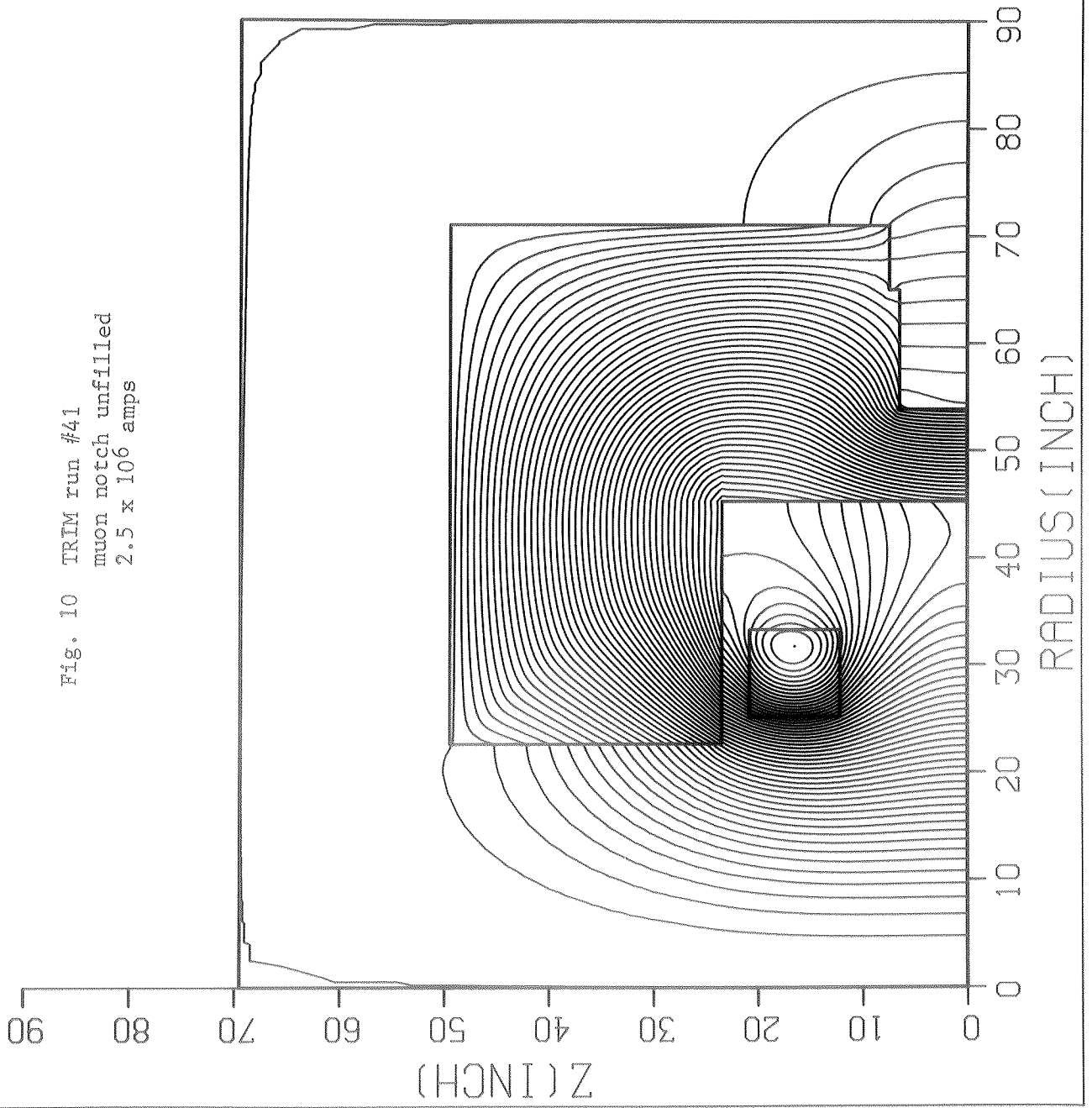


Fig. 11 TRIM run #47
muon notch filled
1.0 x 10⁶ amps

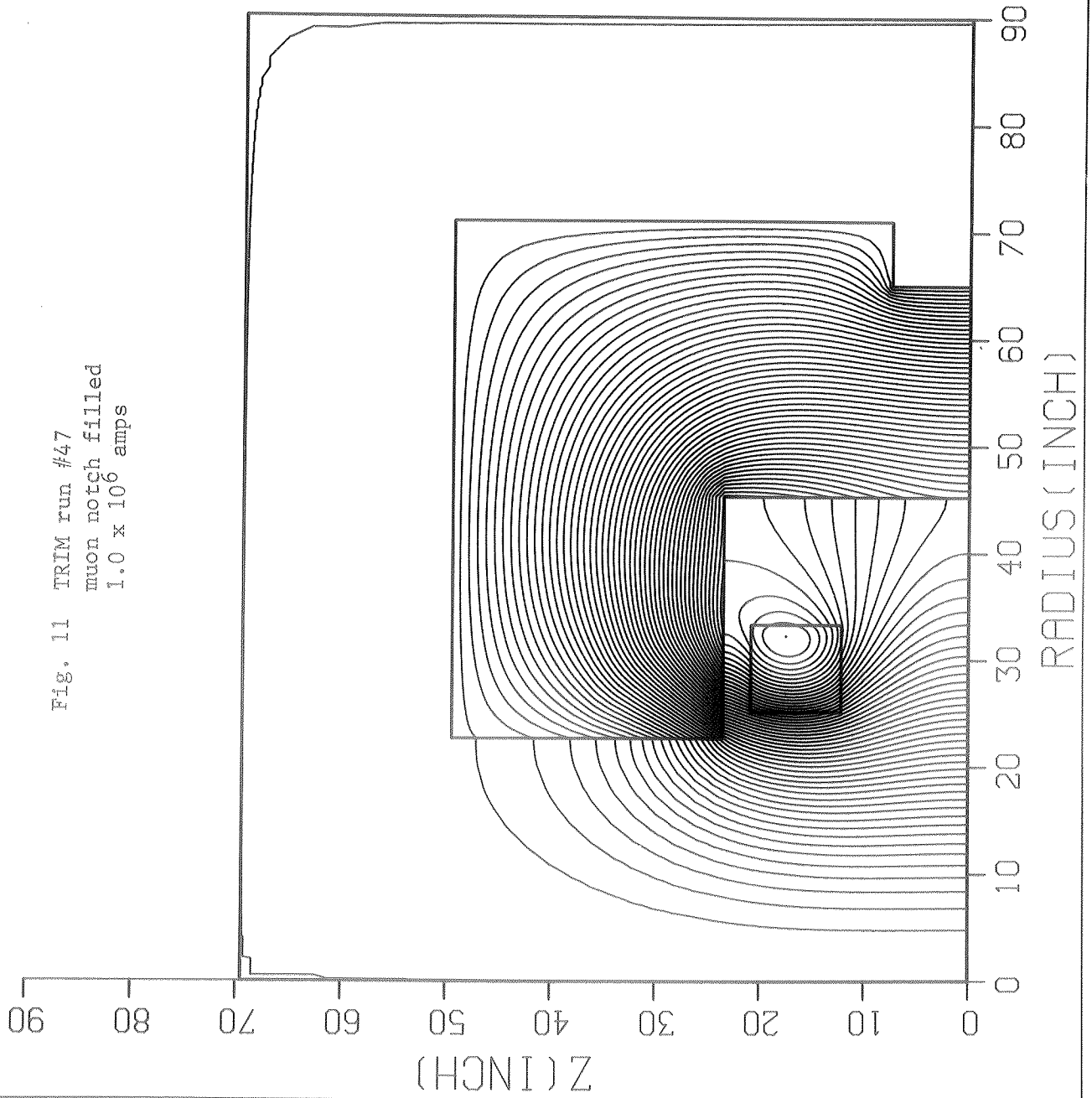
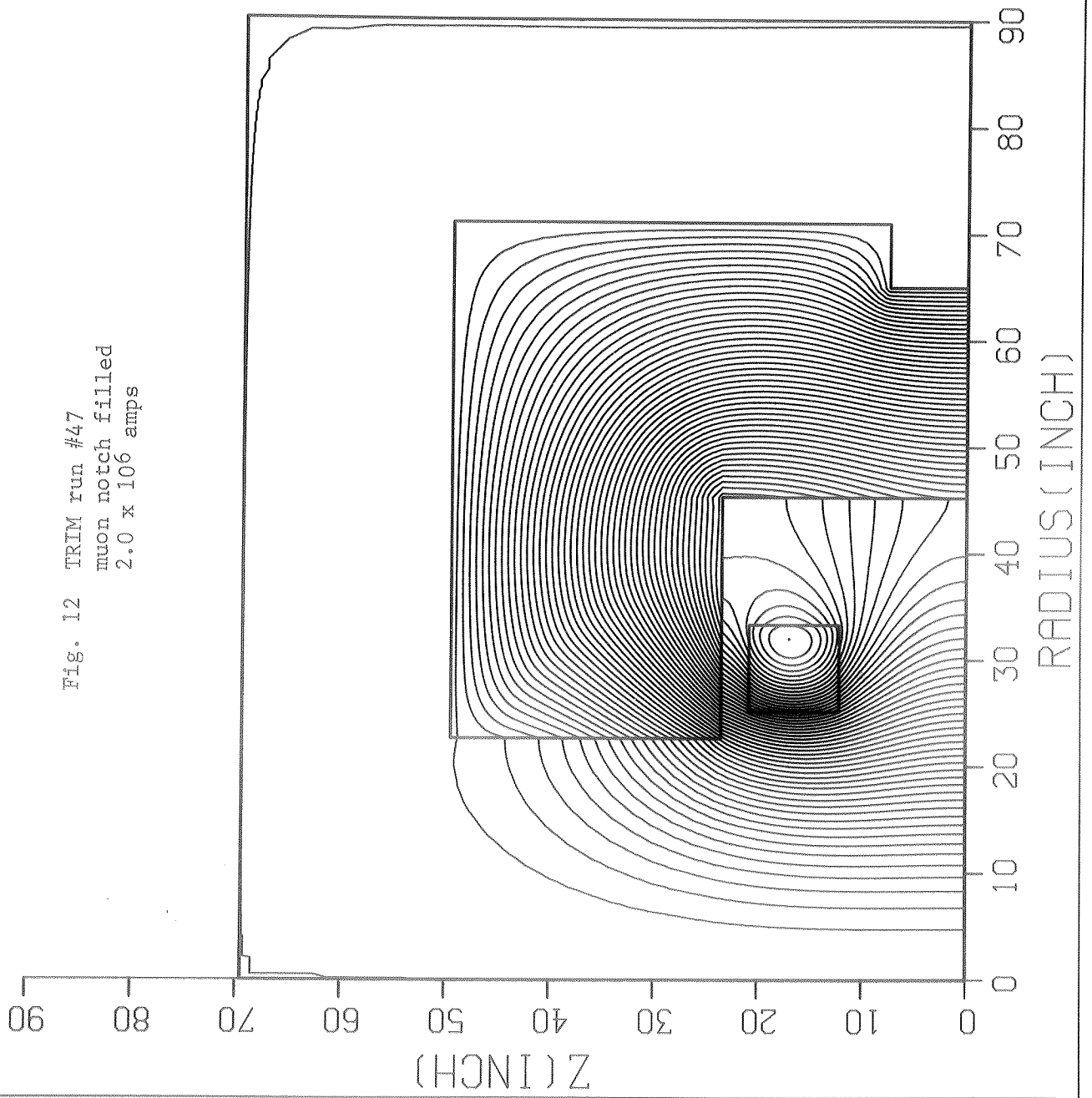


Fig. 12 TRIM run #47
muon notch filled
2.0 x 10⁶ amps



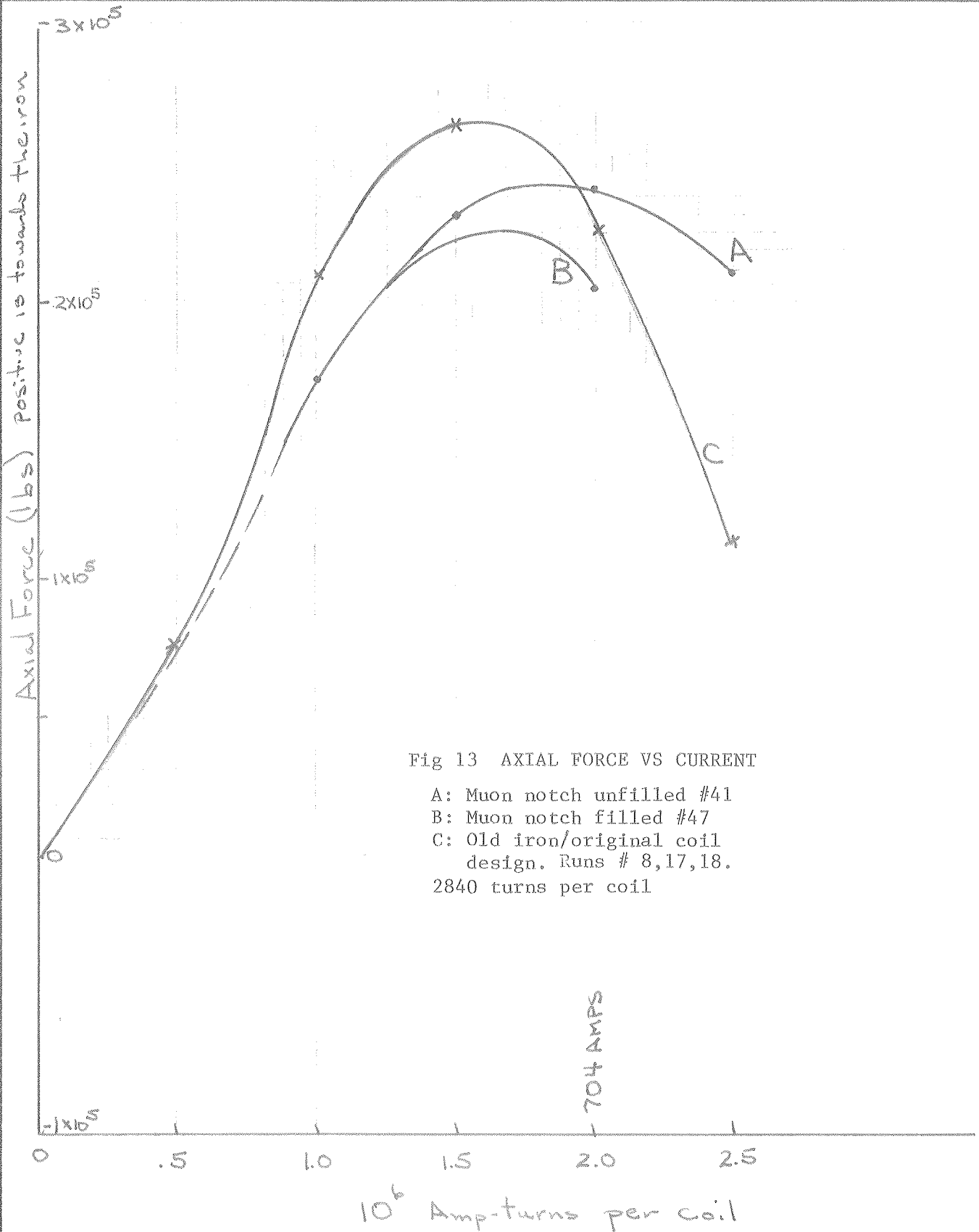


SUBJECT

NAME

DATE

REVISION DATE





SUBJECT

NAME

DATE

REVISION DATE

Fig. 14 AXIAL FORCE VS
COIL LOCATION
Old Iron

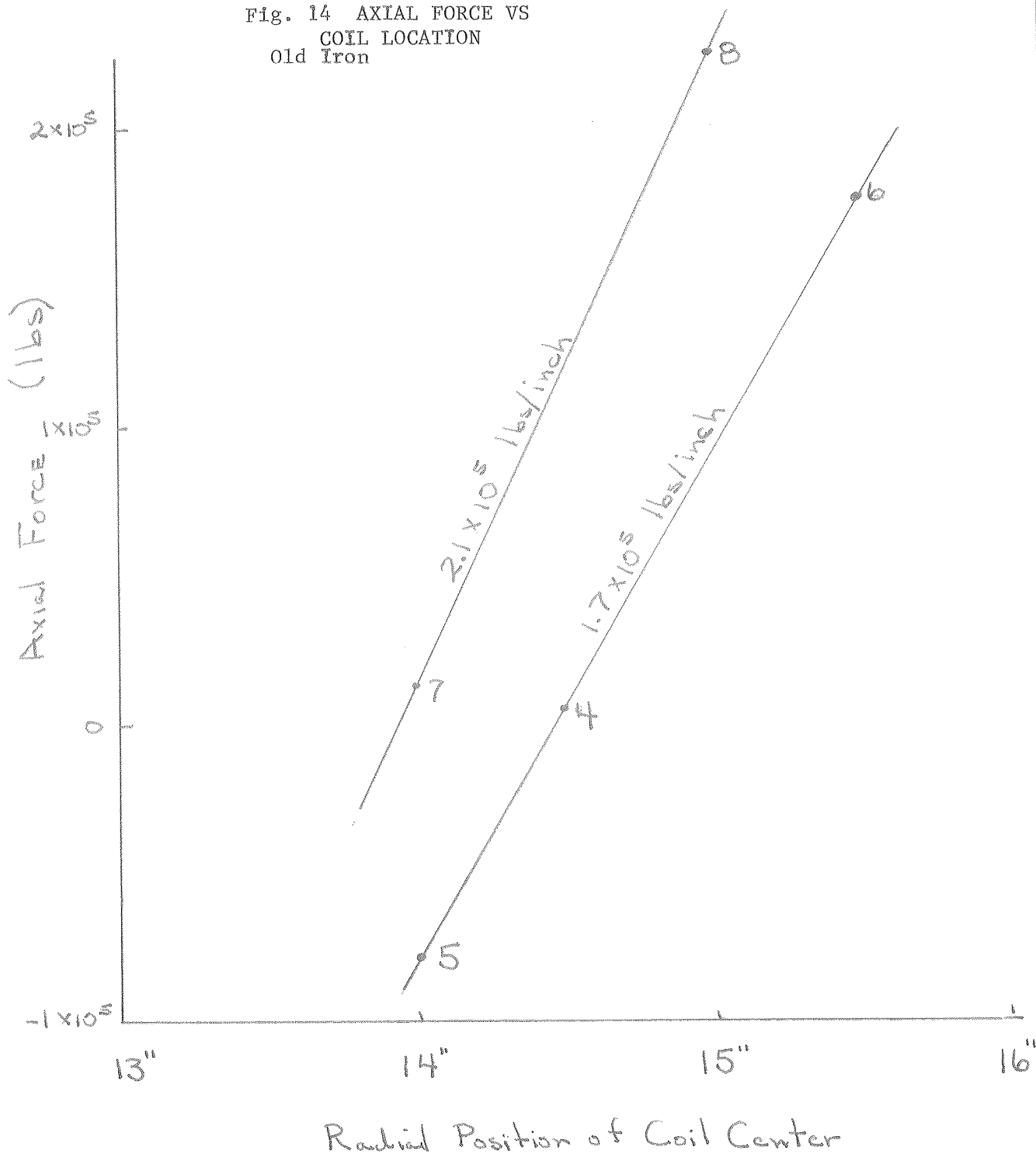
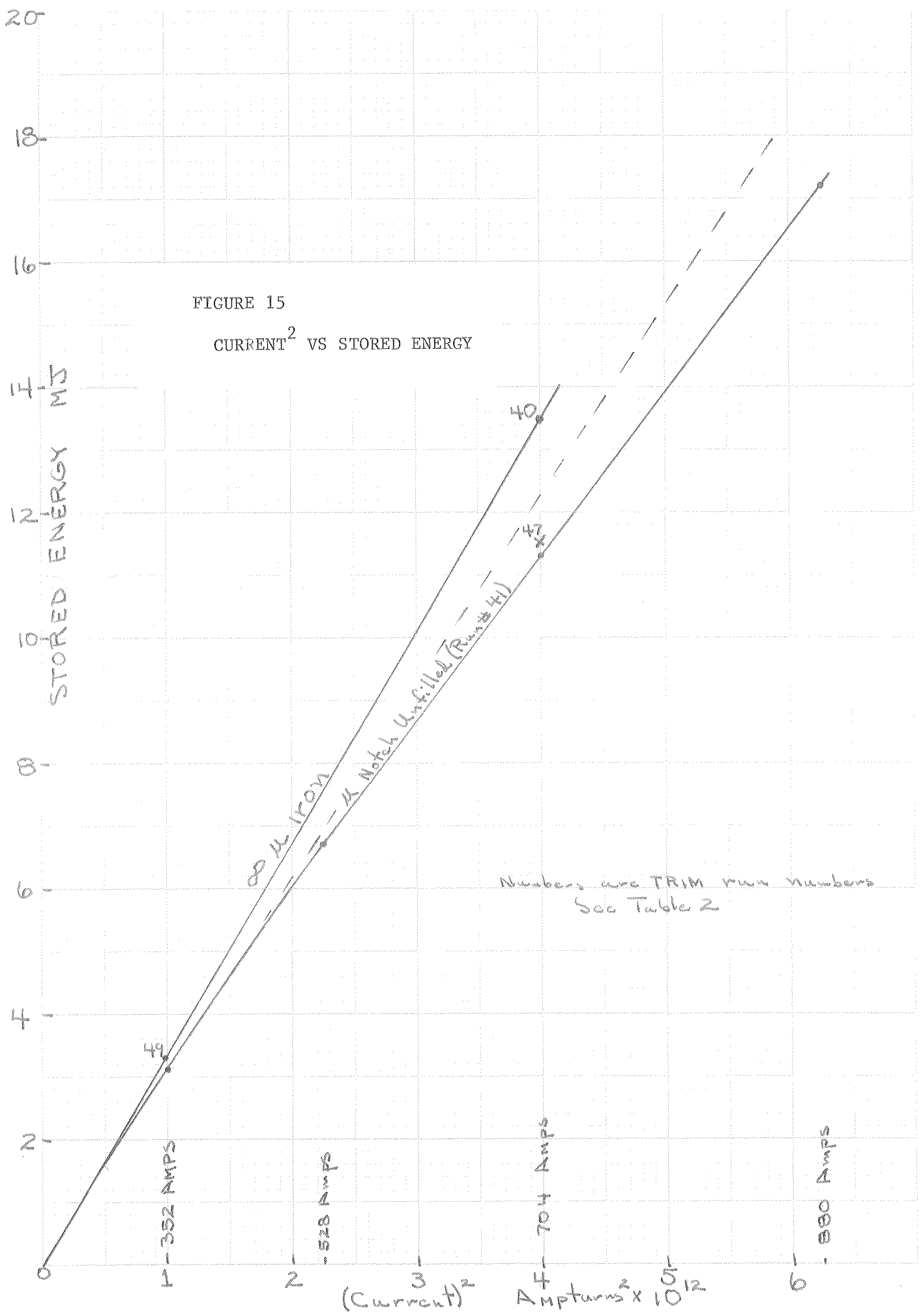


FIGURE 15
CURRENT² VS STORED ENERGY

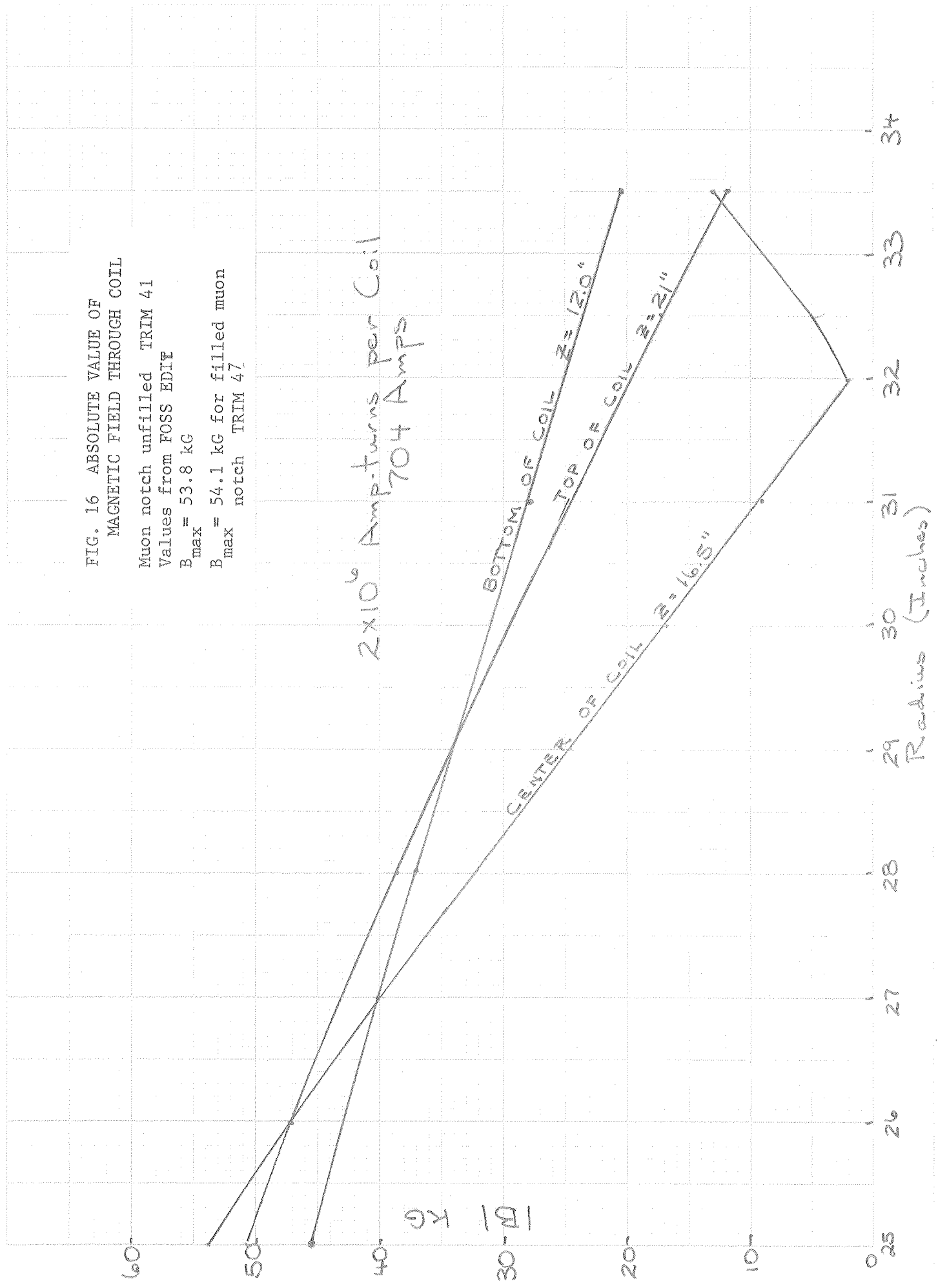


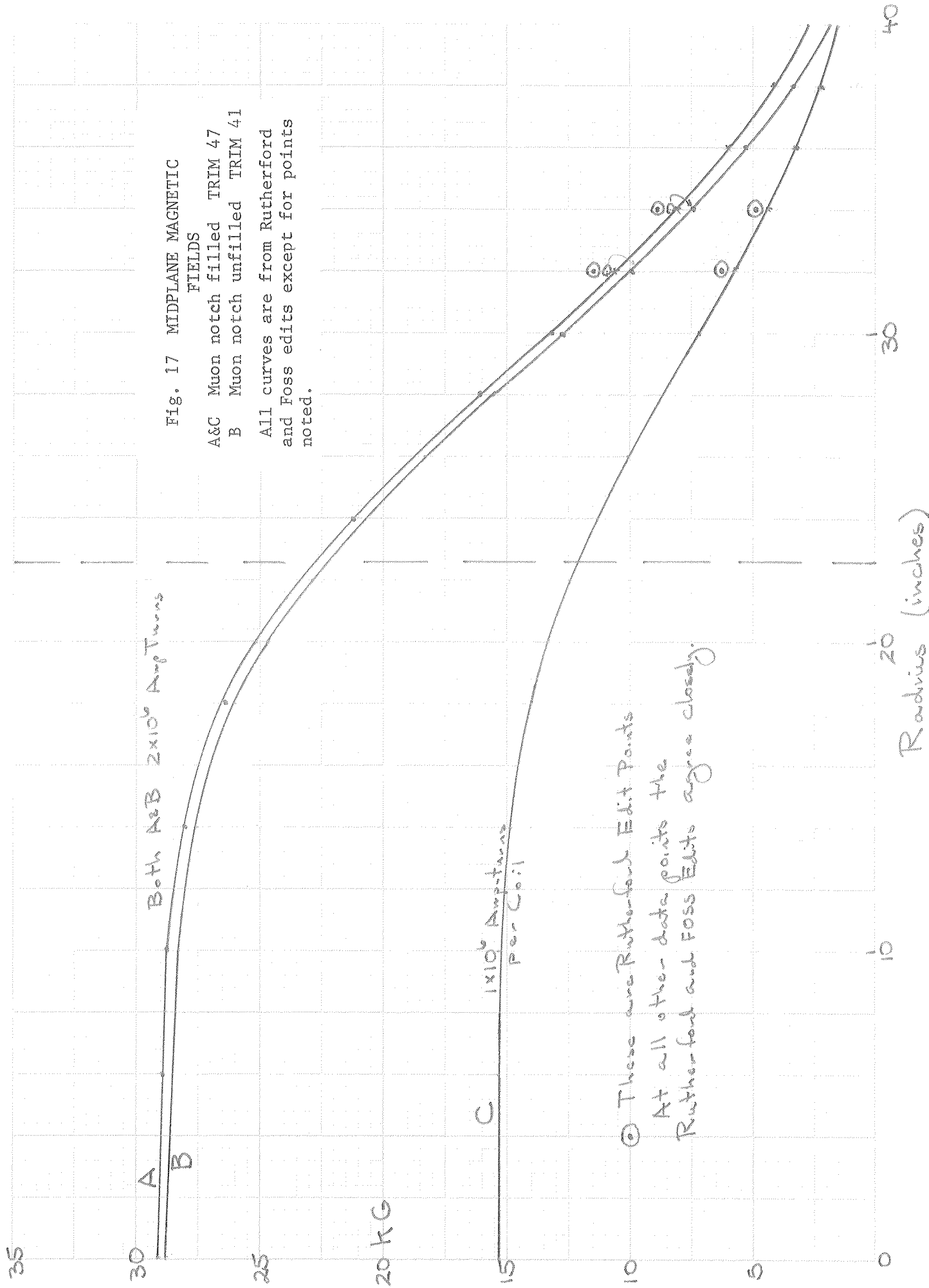
Numbers are TRIM run numbers
See Table 2

FIG. 16 ABSOLUTE VALUE OF
MAGNETIC FIELD THROUGH COIL

Muon notch unfilled TRIM 41
Values from FOSS EDIT
 $B_{max} = 53.8 \text{ kG}$
 $B_{max} = 54.1 \text{ kG}$ for filled muon
notch TRIM 47

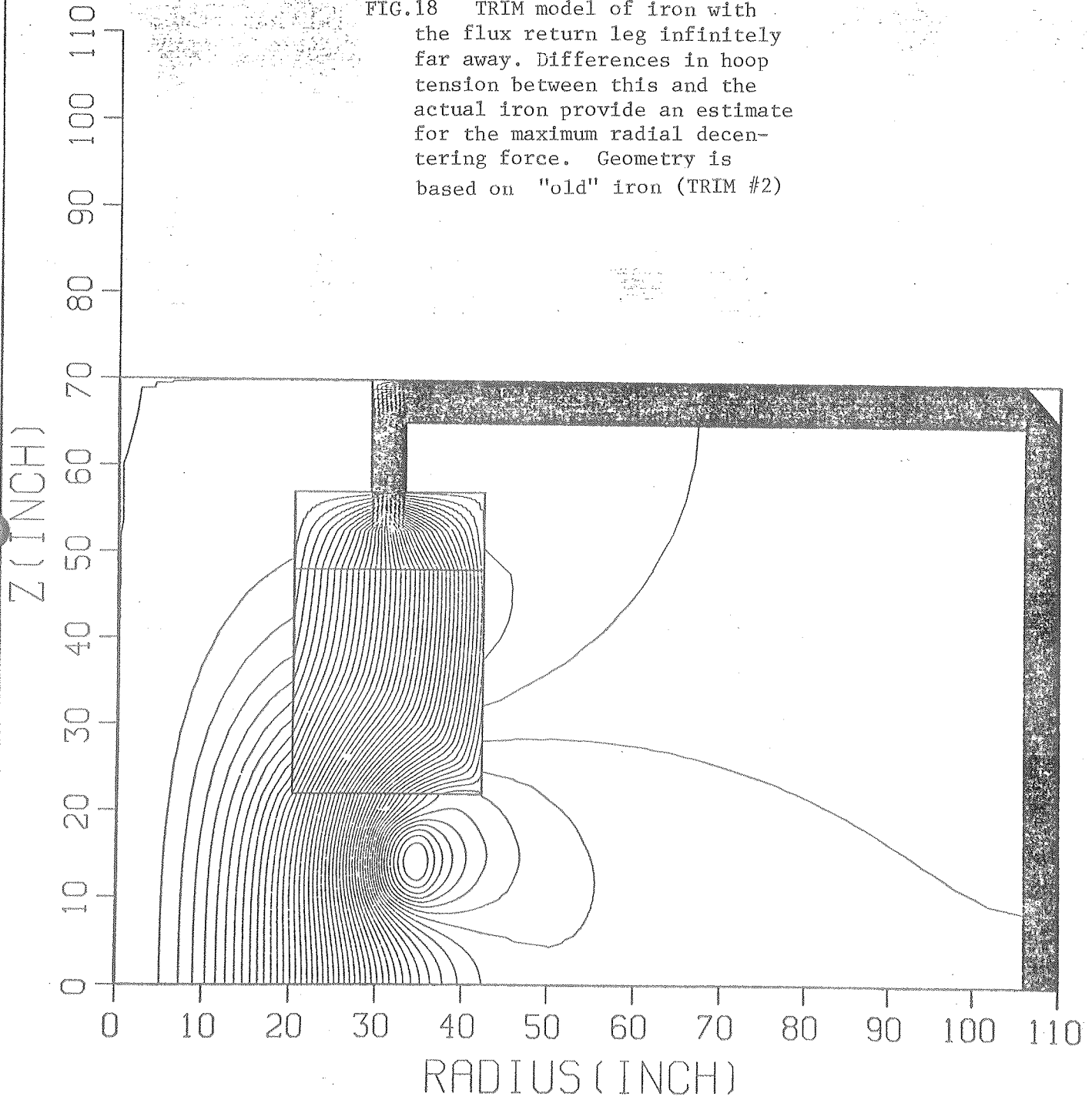
2×10^6 Amp-turns per Coil
704 Amps





BC 34

FIG.18 TRIM model of iron with the flux return leg infinitely far away. Differences in hoop tension between this and the actual iron provide an estimate for the maximum radial decentering force. Geometry is based on "old" iron (TRIM #2)



Measurement of 30" Chamber Magnetic Field

1. A horizontal line was determined and drawn, passing through the geometric center of the coil starting at the back. It was placed on the right hand inside surface of the vacuum box. It was found to correspond to a previously scribed construction line which had presumably been made when the vacuum box was built.
2. A second horizontal line, the magnetic center line, was independently determined by measuring the magnetic field at two corresponding points (points aa) located approximately nine inches above and below the mid-line, and about nine inches out from the inner circumference of the coil. The field in the region is, by previous measurements, expected to be symmetric above and below the mid-line. By making small shifts in location and angle, a pair of measurements (17.75 + 17.35 Kgauss) were obtained. The measurements were repeatable (as were all others) to ± 50 gauss. The field differs in the region by 2.3% with the bottom being stronger. A second set of readings 12" above and below the mid-line yielded fields of 16.69 + 16.34 Kgauss, a difference of 2.1%, consistent with the first set. *(field map is asymptotic up-down by ~2%)*
3. The lines in 1 and 2 were then compared. They were parallel to 0.2 degrees, and separated by 1/16". Then the magnetic and geometric mid-lines of the chamber are essentially the same.
4. A series of field measurements were made along the mid-line from the outside to the inside circumference. The field varied from 340 gauss to 26450 gauss, with a current of 15000 amps in the magnet. The gradient is about 1100 gauss/inch.
5. Measurements were made at locations bb and cc at 11,000, 13,000 and 15,000 amps. Normal operating current is 14,700 for 25 Kgauss at the center of the chamber.
 - i) All field measurements have been made flat against the inside wall of the vacuum box, 1 inch from the coil face.
 - ii) Points bb are located at 26" above and below the mid-line, and 15" downstream of a line through the vertical center of the coil (see fig.). This corresponds to an r, θ of 30.6", $\pm 61^\circ$ from the center of the coil.
 - iii) Points cc are located at 26" above and below the mid-line, and 21.75" downstream of a line through the vertical center of the coil. This corresponds to an r, θ of 34.6", $\pm 50.5^\circ$ from the center of the coil.

The corresponding points are in symmetric locations to better than .1", but their true locations in space are known to no better than $\pm .5$ ".

6. Magnetic measurements at bb and cc:

		B (Kgauss)	<u>up</u>	<u>down</u>	<u>% difference</u>
bb	I = 11000		13.99	14.64	4.5
	13000		16.09	16.79	4.3
	15000		18.11	18.96	4.6
cc	I = 11000		11.05	11.29	2.1
	13000		12.97	13.09	0.9
	15000		14.53	14.75	1.5

The differences are consistently within independent within the 10% range

October 1979

Forces on Current Elements Inside a Spherical Cavity

S. H. Oh and I. A. Pless

In order to estimate radial forces on magnet coils which are embedded in iron, one can try to use the method of images. One geometry for which a closed form solution exists is that of a spherical cavity embedded in an infinite volume of iron which has infinite permeability (i. e. the field inside the iron is zero).

The model of a cylindrical magnet that we will use is illustrated in the following figure:

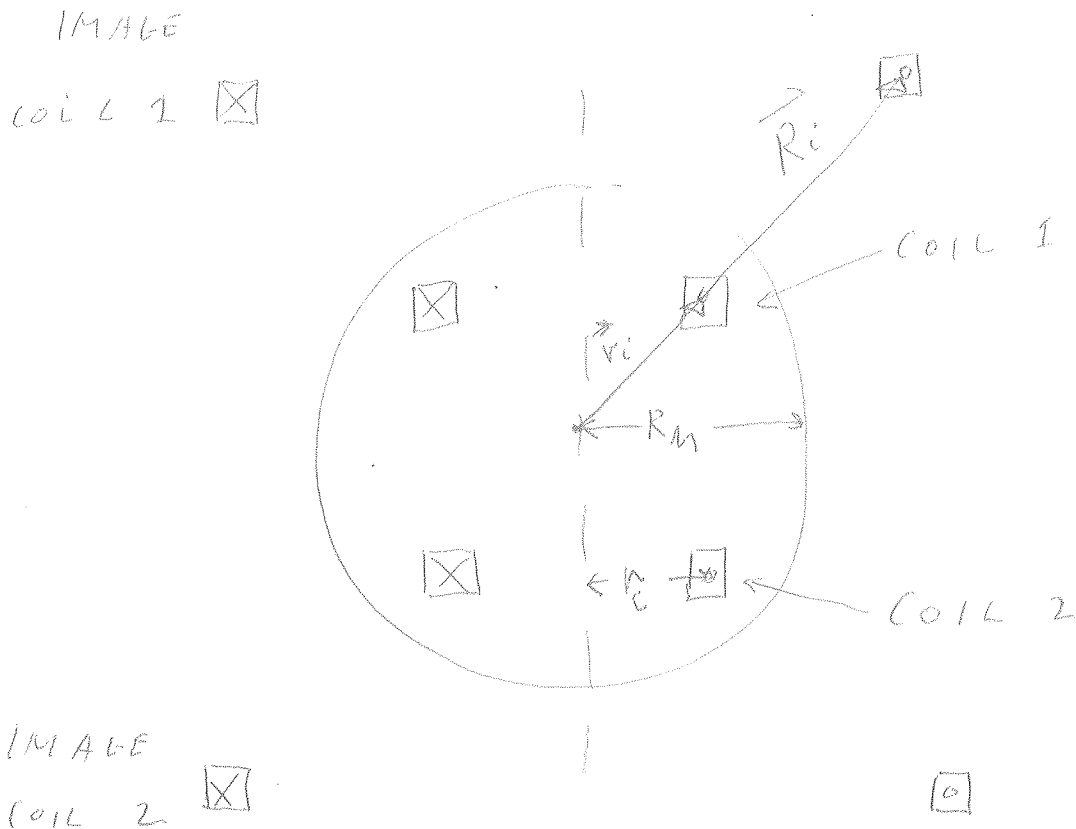


Figure 1

Using the model shown in Figure 1, the problem is to locate the images of the current elements of coils 1 and 2. Once this is done, one can calculate all radial forces due to misalignments. If we express the position of any current element carrying a current i in spherical polar coordinates, we define

$\vec{r}(i) = \hat{r}(\theta_i, \phi_i) r_i$ where $\hat{r}(\theta_i, \phi_i)$ is a unit vector pointing in the direction of $\vec{r}(i)$ and $r_i = |\vec{r}(i)|$.

It is easy to show that all boundary conditions are satisfied if the image of $\vec{r}(i) = \vec{R}(i)$ is given by:

$$\vec{R}(i) = \hat{r}(\theta_i, \phi_i) \frac{Rm^2}{r_i}, \quad (1)$$

(where R_m is the radius of the spherical cavity),

and the image current $= I_i$ is given by:

$$I_i = i \frac{Rm}{r_i}. \quad (2)$$

The direction of the current I_i (or more properly the current density) is given by the tangent to the curve swept out by $\vec{R}(i)$. Although equations (1) and (2) are very simple, the actual use of them is tedious due to the asymmetric geometry once the centers of the two coils have arbitrary relations to the center of the spherical

cavity. However, it is possible to calculate all forces on the coils 1 and 2 by use of these two equations and Biot - Savart's law. While this model should give a reasonable estimate of the radial forces on the coils due to coil misalignments, the calculation of the axial forces could be seriously in error and this estimate of the axial forces will be smaller than the actual forces. To calculate axial forces, it would be better to use the images of the coils in two infinite parallel iron planes.

As an example of the use of equations 1 and 2, we will try to estimate the radial forces on the FHS magnet due to misalignments. In other words, we will try to estimate the radial magnetic force. The model is shown in the next figure.

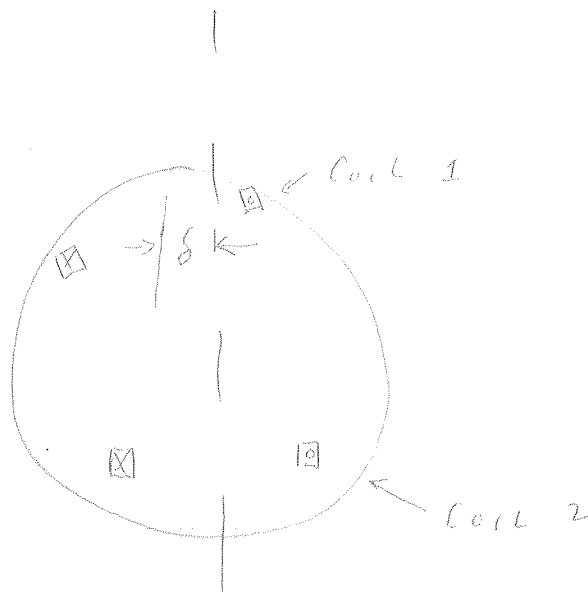


Figure 2

Coil 1 is displaced by an amount δ and its image is also displaced, not only laterally, but also the plane of the coil is tilted. However, to get an estimate of this complicated case, we examine the following model:

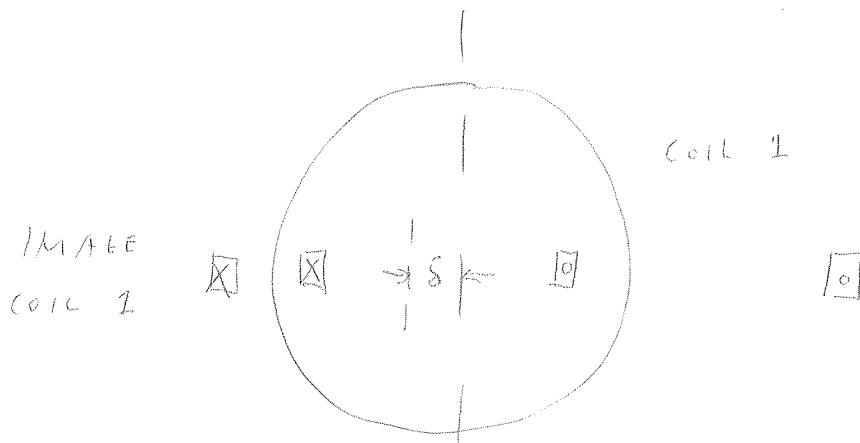


Figure 3

In this model, we have only one coil, and the plane of the coil is in an equatorial plane, and therefore so is its image. This model should overestimate the radial forces on coil 1. The reasons are twofold. First, coil 2 has an attractive effect on coil 1, trying to return it back to the symmetric radial position. The image of coil 2 has the opposite tendency, but since it is further away, the overall effect of coil 2 and its image is to apply a restoring force opposite to the displacement δ . In the geometry of figure 2, the force between coil 1 and its image has both radial and axial components. In figure 3, all forces are radial. If R_m is chosen to be the actual radial distance from the center of coil 1 and the iron, the model in figure 3 should give an overestimate of the radial force on coil 1.

In our calculation we have divided the current in coil 1 into 360 equal current elements. Then, using equations 1 and 2, the images of these current elements were calculated. Using Biot-Savart's Law, the magnetic force on a particular current element of coil 1 due to these 360 image currents was then summed. Finally the magnetic force on the 360 current elements of coil 1 was summed to yield the force on coil 1. For a fixed radius r_c , the force was practically a linear function of the displacement δ (δ in the range 0-2 inches), allowing the calculation of a force constant K. The results are summarized below.

The following data is relevant for the FHS magnet.

$$R_m = 45.25 \text{ inches}$$

r_c can vary from 26" to 28".

$$i = 1.5 \times 10^6 \text{ amperes}$$

The following table is our estimate of the radial magnetic force constant K as a function of r_c .

r_c	K(pounds/inch (displacement))
26	9,923
28	13,840
30	19,610
32	28,500
34	42,990

Subject

PROGRESS REPORT ON THE 30" HYDROGEN
BUBBLE CHAMBERName
J. Mark/W. WalkerDate
May 10, 1962MAGNET COMPONENTS

The iron yoke for the magnet has been delivered. The Allis Chalmers Company of Milwaukee did the machining on steel supplied by the U. S. Steel Company. The steel composition specified was carbon, .08% max.; manganese, 0.5% max.; phosphorus, .04% max.; sulphur, 0.5% max., nickel, 0.15% max., chromium, 0.12% max., molybdenum, .03% max., copper, 0.2% max., iron to be not less than 98.80%. Average grain size is .002" or larger, and all pieces were forged, bloomed, or rolled.

The copper coils were fabricated by the General Electric Company of North Bergen, New Jersey. We purchased nine "pancakes" in order to have one spare. Each pancake is about 4 inches thick, 95 inches outside diameter, 40 inches inside diameter, and weighs about 4,200 pounds. Each pancake consists of 25 turns of hollow copper conductor 1.85 inches square with a 1.042" diameter hole through it. The coils are insulated with fiberglass tape and vacuum impregnated with epoxy resin. The pancakes will be connected electrically in series with 8 water circuits requiring about 400 gallons per minute total when running at full excitation of 20,000 amps at 250 volts.

The coils did not quite meet the tolerances as to flatness. In order to prevent warpage of the coils when under full power, it will probably be necessary to shim slightly between coils. Calculations by A. Peekna show that there are large magnetic forces (approximately 100 psi) acting on the individual coils. These must be balanced mechanically by means of shimming.

Figure 2 shows the magnet. Notice the ball joint between the jack and the floor pad. The ball joint insures that the pad and floor plates are parallel. By pumping grease through 100 small holes in each of the 8 feet we can float all of the magnet for purposes of changing locations. For separating the two halves of the magnet, the feet on the moving half will be pressurized. Small scale tests indicate that the coefficient of friction for this system is less than 1%. When the magnet is moved to the end of a floor plate, more travel will be possible by lowering the magnet to the floor and raising the feet up so the plates can be moved to another position. In this manner the magnet can move wherever we can provide a strong flat floor.

Initial tests on moving the magnet blocks were made using thin aluminum plates, laid directly on the floor. Unfortunately, the floor was not sufficiently flat so that the skids gouged the aluminum. We now have two inch plates of steel with sufficient strength and flatness to provide a suitable surface for skidding.

We have designed a lubricated turntable to make it easy to rotate the bubble chamber magnet. After we gain experience using the other system, the decision whether or not to build it will be made. Jacks are used to raise and lower the magnet.